IEEE/CSC & ESAS SUPERCONDUCTIVITY NEWS FORUM (global edition), January 2015.
ASC 2014 manuscript 1MOr3C-05 published online in *IEEE Trans. Appl. Supercond. (IEEE XPLORE)*
DOI: 10.1109/TASC.2014.2368072 on November 4, 2014.

Optimizing Flux Pinning of $YBa_2Cu_3O_{7-\delta}$ (YBCO) Thin Films with Unique Large Nanoparticle Size and High Concentration of Y_2BaCuO_5 (Y211) Additions

Mary Ann P. Sebastian[1], Joshua N. Reichart[1], Margaret M. Ratcliff[1], Jack L. Burke [2], Timothy J. Haugan[1]
Chen-Fong Tsai[3], Haiyan Wang[3]

***Abstract*—Addition of second-phase nanosize defects to $YBa_2Cu_3O_{7-\delta}$ (YBCO) superconductor thin films is known to enhance flux pinning and increase current densities (J_c). The addition of Y_2BaCuO_5 (Y211) was studied previously in $(Y211/YBCO)_N$ multilayer structures, and in Y211+YBCO films deposited from pie-shaped targets. This research systematically studies the effect of Y211 addition in thin films deposited by pulsed laser deposition from $YBCO_{1-x}Y211_x$ (x = 0-20 vol. %) single targets, at temperatures of 785 - 840 °C. Interestingly, the resulting size of Y211 particles is 20 to 40 nm, in contrast to 10 to 15 nm in previous studies of Y211 and 5-10 nm for other 2nd-phase defect additions; and the number density is reduced. A slight increase of $J_c(H,T)$ was achieved, compared to previous optimization studies. Results and comparisons of flux pinning, intrinsic stresses imaged by TEM, current densities, critical temperatures, and microstructures will be presented. The overall low intrinsic stress on YBCO from Y211 lattice mismatch is smaller than previously studied 2nd-phase defect additions known, which is hypothesized to be the driving force in achieving the unusually large 2nd-phase nanoparticle size and volume fraction thus-far in YBCO thin films.**

***Index Terms*— Critical current density, Flux pinning, High-temperature superconductors, Yttrium barium copper oxide**

I. Introduction

Addition of nano-sized second-phase inclusions to $YBa_2Cu_3O_7$ (YBCO) superconducting thin films enhances flux pinning, resulting in an increase in current densities (J_c) [1]-[24]. Previous studies conducted have focused on single phase additions of many materials including: Y211 nanoparticles, Y_2O_3 nanoparticles, $BaSnO_3$ (BSO) nanorods, Ba_2YNbO_6 (BYNO) nanorods, and $BaZrO_3$ (BZO) nanoparticles or nanorods [2]-[9]. Research has also focused on combining the artificial pinning centers resulting from BZO nanorods and Y_2O_3 nanoparticles [11],[12] and BSO nanorods and Y_2O_3 nanoparticles [13], [14]. These nano-sized additions are accomplished through various pulsed laser deposition (PLD) techniques: including the use of a mixed target composition, the use of individual targets with a multilayer PLD technique, and the use of a mixed YBCO and 2nd phase target with the addition of a pie sector incorporating Y_2O_3, and incorporating decorated substrates [1]-[24].

Nanophase additions can also be classified as one, two, and three dimensional artificial pinning centers (1D - APC, 2D - APC, 3D - APC), with 1D - APC's displaying linear defects such as BSO and BZO nanorods. Nanosize 2D – APC's display planar defects, and include "... small angle grain boundaries, anti-phase boundaries, and surfaces of large precipitates." Nanosize 3D – APC's result from nanoparticles, such as Y_2O_3 and Y211 [6].

In particular, the 3D-APC of Y211 exhibits a smaller overall average lattice mismatch with YBCO, when compared to other inclusions, such as Y_2O_3, BSO, and BZO, as evidenced in Table 1. The low degree of mismatch lends to sharper interfaces between the Y211 nanoparticles and the epitaxial YBCO film.

Past research showed that doping targets of YBCO with 1.6 wt. % Y211 nanoparticles resulted in thin films with slightly higher current J_c at higher fields than pure YBCO films [17]. Previous research also confirmed that Y211 nanoparticles at 5 vol. % prove to be efficient and strong 3D pinning centers throughout the film thickness [18], [19]. Y211 nanoparticles have been included in thin films by pulsed laser deposition of single targets consisting of YBCO and Y211, and as multilayer films by alternating targets of YBCO and Y211 during the deposition [20] - [24]. While the Y211 multilayer films produced better pinning at fields less than 3 – 4 T, the simplicity of Y211 doping of a single target in PLD thin films for enhancing pinning is attractive [21]. It is of interest to investigate and optimize the addition of various volume percent of Y211 on flux pinning, current densities, and induced strain in YBCO thin films.

Manuscript received August 1, 2014. This work was supported in part by AFRL Aerospace Systems Directorate (RQQM) and the Air Force Office of Scientific Research (AFOSR)

M. A. Sebastian is with Air Force Research Laboratory, RQQM, Wright Patterson A.F.B., OH 45431 USA, phone: 937-255-5930; e-mail: mary_ann.sebastian@us.af.mil.

T. J. Haugan is with Air Force Research Laboratory, RQQM, Wright Patterson A.F.B., OH 45431 USA , e-mail Timothy.Haugan@us.af.mil.

J. N. Reichart was with Air Force Research Laboratory, RQQM, Wright Patterson A.F.B., OH 45431 USA, e-mail: jnreichart@gmail.com.

M. M. Ratcliff was with Air Force Research Laboratory, RQQM, Wright Patterson A.F.B., OH 45431 USA, email: Margaret.Ratcliff@us.af.mil.

J. L. Burke was with UDRI, University of Dayton, OH 45469 USA, e-mail: Jack.Burke@us.af.mil.

C. F. Tsai was with Materials Science and Engineering Program Texas A&M, College Station, TX 77843 USA, e-mail seraphwing@neo.tamu.edu.

H. Wang is with Materials Science and Engineering Program Texas A&M, College Station, TX 77843 USA, e-mail: wangh@ece.tamu.edu

IEEE/CSC & ESAS SUPERCONDUCTIVITY NEWS FORUM (global edition), January 2015.
ASC 2014 manuscript 1MOr3C-05 published online in *IEEE Trans. Appl. Supercond. (IEEE XPLORE)*
DOI: 10.1109/TASC.2014.2368072 on November 4, 2014.

TABLE I
LATTICE PARAMETERS AND CORRESPONDING LATTICE MISMATCH OF YBCO, Y211, Y_2O_3, AND BZO [25,26].

	Lattice Parameter Å	Lattice Mismatch to YBCO wrt ab-avg	Lattice Mismatch to YBCO wrt c-axis	Overall Avg. Mismatch
YBCO	a = 3.825 b = 3.886 c = 11.66			
Y211[a]	a = 7.132 b = 12.18 c = 5.659	$Y211_a$ / $YBCO_{ab\text{-}avg}$ = -7.5% $Y211_c$ / $YBCO_{ab\text{-}avg}$ = -2.1%	$Y211_b$ / $YBCO_c$ = 4.5%	-0.15%
Y_2O_3	10.604	-2.8%	-9.1%	-5.6%
BZO	4.193	8.8%	7.9%	8.3%

a. Nanosize Y211 orientation $Y211_{b\text{-}axis}/YBCO_{c\text{-}axis}$ in $[Y211/YBCO]_N$ multilayer films [23].

I. Experimental

Targets were produced via solid state processing of commercial powders of $YBa_2Cu_3O_{7-\delta}$ (YBCO) and Y_2BaCuO_5 (Y211). Powders were dried in a furnace for 8 hours at 450 °C. The dried powders were measured and mixed with an agate mortar and pestle to comprise compositions of 5, 7.5, 10, 12.5, 15, and 20 vol.% Y211, with the remaining volume percent YBCO. The mixtures were then individually pressed utilizing a 1.25 inch die and a pressure of 1000 psi. The targets were then sintered at 850 °C for 60 hours and 920 °C for 156 hours. Final densities of the targets ranged between 87% and 93%. Thin films were produced using pulsed laser deposition on $LaAlO_3$ (LAO) and $SrTiO_3$ (STO) single crystal substrates. A Lambda Physik LPX 300 KrF excimer laser (λ=248nm) with a fluence of approximately 3 J/cm^2, was utilized for the depositions. Laser deposition parameters utilized were laser energy of 450 mJ, repetition rates of 2, 4, and 6 hz, and a chamber atmosphere of 300 mTorr oxygen. Deposition temperature was varied between 785 °C and 840 °C to determine optimal conditions. After deposition, the films were annealed at 500 °C in an oxygen atmosphere for a 30 minute dwell time. Deposition time of 18 minutes produced film thicknesses of 250-325 nm. Current density and critical transition temperature were measured with a Quantum Design Physical Properties Measurement System (PPMS) with a vibrating sample magnetometer (VSM) probe. The VSM data was attained for conditions of 77 K, 65 K, 20 K, and 5 K with an applied field varied from 0-9 T for H // c-axis of the films. A FEI Sirion Scanning Electron Microscope (SEM) with ultra-high resolution at 5 kV and a spot size of 3 was used to obtain images of the films' surface. Cross-sectional Transmission Electron Microscopy (XTEM) images and Scanning Transmission Electron Microscopy image (STEM) were obtained using a FEI Tecnai F20 analytical microscope under the acceleration voltage of 200 kV. Lattice parameters were determined by x-ray diffraction analysis utilizing a Rigaku DMAX 2500.

II. Results

From Fig. 1(a), (b): experimental data shows optimized $J_c(H)$ for H < 6 T at 65 K for a deposition temperature of 835-840 ˚C and a repetition rate of 4 hz respectively, for the optimal composition of 10 vol. % Y211. Fig. 1(c) depicts current density as a function of applied field for 5 K and 65 K, and illustrates that the pinning advantage and increased current densities resulting from the addition of 10 vol. % Y211 is maintained regardless of the applied field ranging from H = 0-8 T, and regardless of the temperature ranging from 5 K to 65 K. The log-log plot shown in Fig. 1(d) results in an α = 0.40 and 0.27 for YBCO and 10% Y211 respectively at 65K with an applied field between H = 0.1 - 1 T; where α is the factor from $J_c \propto H^{\alpha}$ [17]. As illustrated in Fig. 2, a $T_{c\text{-}onset}$ temperature of 89.7 K for the optimized films was attained from zero-field-cooled measurements via the VSM-PPMS, and is comparable to that of pure YBCO films.

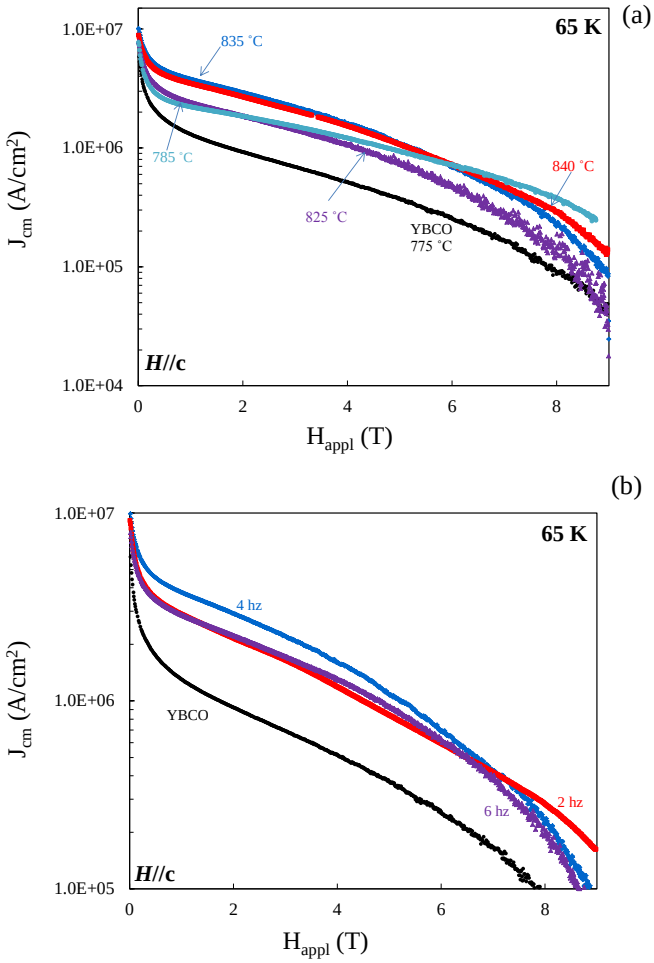

Fig. 1(a),(b). Current density as a function of applied field for YBCO with 10 vol. % Y211 measured at 65K for: (a) films deposited at deposition temperatures ranging from 775 – 840 °C, (b) films deposited at repetition rates of 2, 4, and 6 hz.

IEEE/CSC & ESAS SUPERCONDUCTIVITY NEWS FORUM (global edition), January 2015.
ASC 2014 manuscript 1MOr3C-05 published online in *IEEE Trans. Appl. Supercond. (IEEE XPLORE)*
DOI: 10.1109/TASC.2014.2368072 on November 4, 2014.

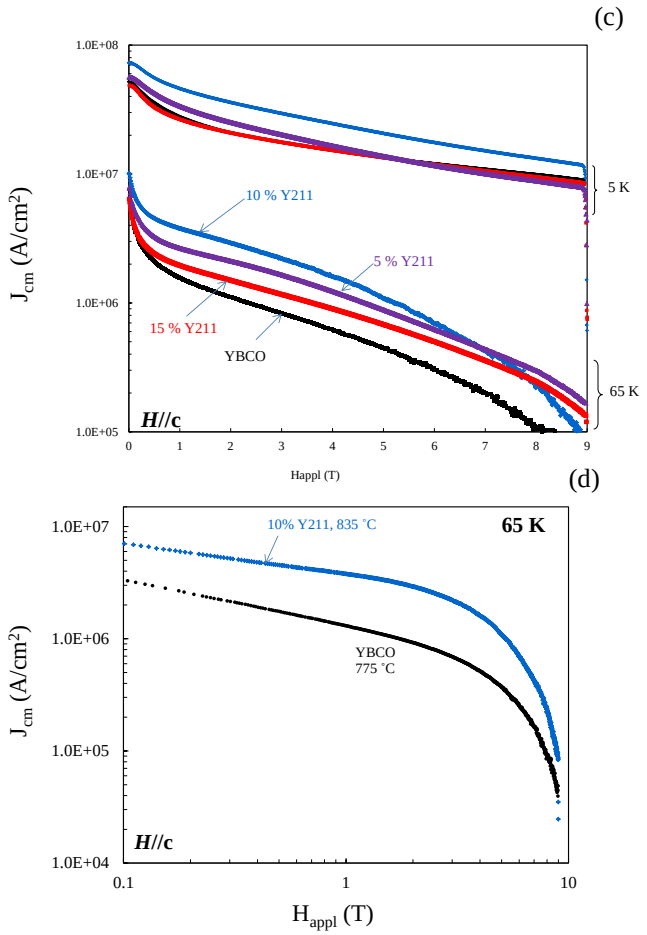

Fig. 1(c),(d). Current density as a function of applied field at 65K and 5K: (c) for various vol. % Y211 additions. (d) log-log plot of current density verses applied field at 65K for YBCO and 10 vol. % Y211 doped YBCO.

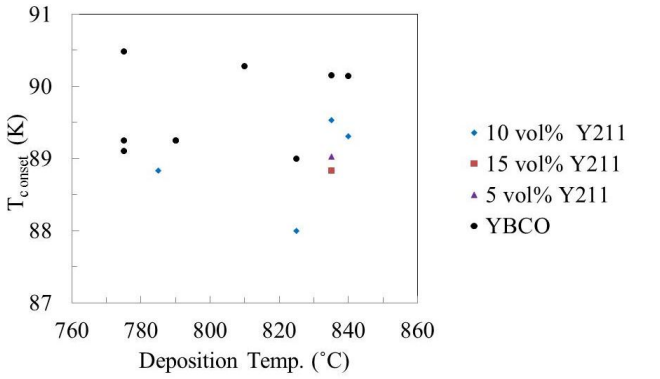

Fig. 2. $T_{c\text{-}onset}$ (K) verses deposition temperature (˚C) for YBCO and various vol. % Y211 additions.

Microstructure studies included both SEM and TEM analysis. Referring to Fig. 3, comparisons of SEM images at 20K and 50K magnification produced from targets composed of composition 5, 7.5, 10, and 12.5 vol. % Y211addition, show the corresponding larger grain sizes, increased pores, and defects changing due to Y211 addition. TEM analysis in Fig. 4 provides comparison of the microstructure of 5 vol. % and 10 vol. % Y211 doped YBCO. TEM micrographs illustrate

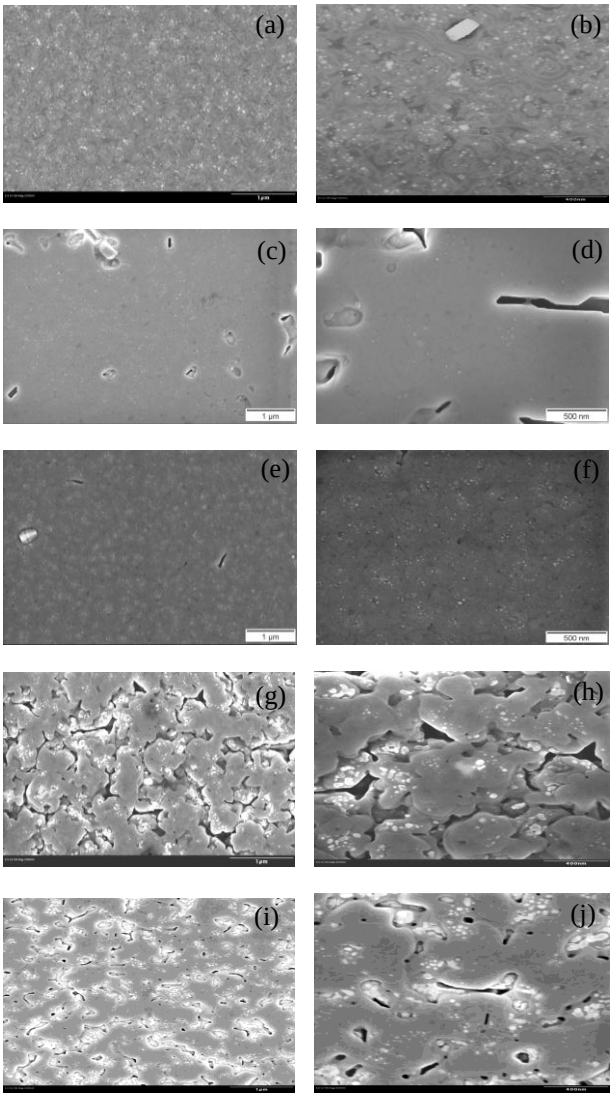

Fig. 3 (a)-(j). SEM images of YBCO and various volume % Y211 doped films on STO substrates at magnifications of 20K and 50K respectively: (a),(b) YBCO deposited at 790˚C. (c), (d) 5 vol.% Y211 deposited at 835 ˚C. (e),(f) 7.5 vol. % Y211 deposited at 835 ˚C. (g), (h) 10 vol.% Y211 deposited at 835 ˚C. (i), (j) 10 vol. % Y211 deposited at 825 ˚C.

remarkable large particle size of 30 to 40 nm. Analysis suggests that the Y211 dopants introduce compressive stress in the YBCO lattice. While misfit dislocations are present in the YBCO lattice, the dislocations predominate in the Y211 phases. Plane buckling and tilting in the YBCO lattice around the Y211 phases may provide additional flux pinning. YBCO lattices appear less stressed as the distance from Y211 particles increases.

Results of x-ray diffraction analysis provide information on the d spacing for the YBCO planes (002), (003), (005), and (006) based on the Bragg equation [26]. The chief source of error with the Hull Debye-Scherrer camera is off centering of the specimen. The Cohen method of extrapolation takes into account the error resulting from displacement of the specimen from the diffraction axis. Graphing the c lattice length for

IEEE/CSC & ESAS SUPERCONDUCTIVITY NEWS FORUM (global edition), January 2015.
ASC 2014 manuscript 1MOr3C-05 published online in *IEEE Trans. Appl. Supercond. (IEEE XPLORE)*
DOI: 10.1109/TASC.2014.2368072 on November 4, 2014.

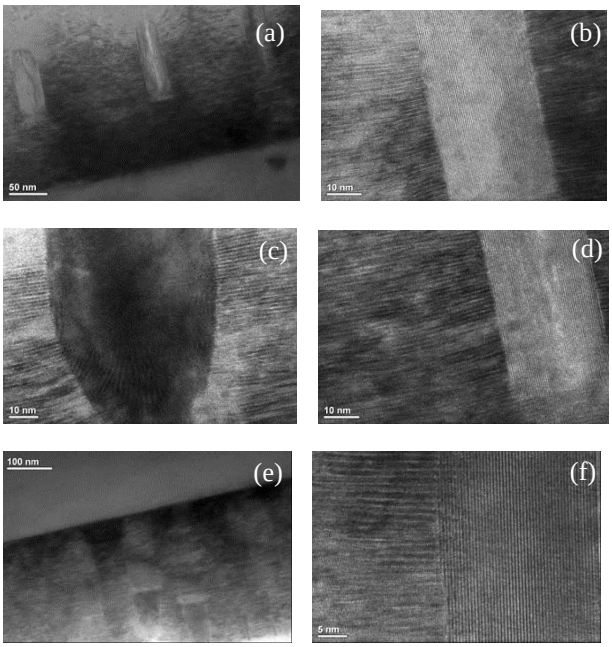

Fig. 4(a)-(f). TEM images of vol.% Y211 doped YBCO films: (a)-(d) 5 vol.% Y211 doped YBCO. (e)-(f) 10 vol. % Y211 doped YBCO.

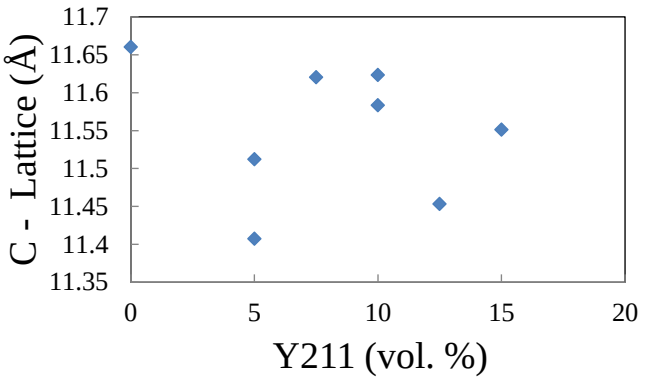

Fig. 5. XRD analysis of YBCO c – lattice parameter verses volume % Y211 doped YBCO.

each plane versus the $\cos^2\Theta/\sin\Theta$ and extrapolating to zero gives the c values [26]. XRD analysis presented in Fig. 5. shows that the c- lattice parameter decreases as the vol. % Y211 increases in the doped YBCO films. This reaffirms the TEM analysis suggesting compressive stresses in the YBCO lattice, which causes the c – lattice parameter to shorten.

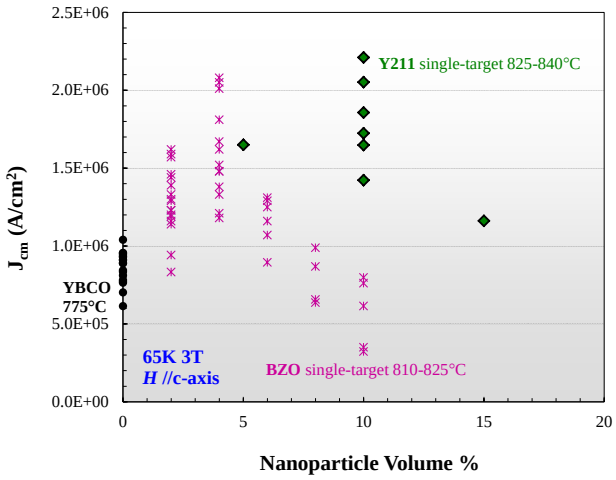

Fig. 6. Comparison of current density verses various volume % of BZO and Y211 doped YBCO films.

III. Conclusion

Experimental results illustrate that a significantly higher percentage of 10 vol. % Y211 can be incorporated into YBCO films without degradation of J_{cm}, in contrast to previous research results from additions of Y_2O_3 and BZO (Fig. 6), [24]. Referring to Fig. 4, TEM analysis illustrates the extraordinary large particle size of 30-40 nm, and that a remarkable clean interface exists between Y211 and YBCO, resulting in less stress in the structure. Future work will measure $J_{ct}(H,T, \theta)$ for θ = 0 to 90°, and explore further TEM analysis to qualitatively and quantitatively determine the effects of Y211 additions on YBCO lattice stresses. The experimental data presented should be helpful for a theoretical investigation of a possible new-regime of collective pinning responsible for the increased pinning of the vortex lattice.

Acknowledgment

The authors wish to acknowledge Ryan Snyder (Air Force Research Laboratory RQQM) for contribution of x-ray diffraction scans.

References

[1] P. Mele, *et al.,* "Incorporation of double artificial pinning centers in $YBa_2Cu_3O_{7-d}$ films," *Supercond. Sci. Technol.,* vol. 21, no.1, 7 pp., 2008.

[2] T. Haugan, *et al.,* "Temperature and magnetic field dependence of critical current density of YBCO with varying flux pinning additions," *IEEE Tran. On Appl. Supercond.*, vol. 19, no.3, pp. 3270-3274, 2009.

[3] C. V. Varanasi, P. N. Barnes, J. Burke, "Enhanced flux pinning force and uniquely shaped flux pinning force plots observed in $YBa_2Cu_3O_{7-x}$ films with $BaSnO_3$ nanoparticles," *Supercond. Sci.Technol.*, vol. 20, no. 10, pp. 1071-1075, 2007.

[4] T. Haugan, *et al.,* "Flux pinning of Y-Ba-Cu-O films doped with $BaZrO_3$ nanoparticles by multilayer and single target methods," *IEEE Trans. on Appl. Supercond.*, vol. 17, no. 2, pp. 3724-3728, June 2007.

IEEE/CSC & ESAS SUPERCONDUCTIVITY NEWS FORUM (global edition), January 2015.
ASC 2014 manuscript 1MOr3C-05 published online in *IEEE Trans. Appl. Supercond. (IEEE XPLORE)*
DOI: 10.1109/TASC.2014.2368072 on November 4, 2014.

[5] P. Mele, *et al.,* "Systematic study of the $BaSnO_3$ insertion effect on the properties of $YBa_2Cu_3O_{7-x}$ films prepared by pulsed laser ablation," *Supercond Sci. Technol*, vol. 21, no. 12, 6 pp., 2008.

[6] K. Matsumoto, P. Mele, "Artificial pinning center technology to enhance vortex pinning in YBCO coated conductors," *Supercond. Sci. Technol.*, vol. 23, no. 1, 12 pp., 2010.

[7] J. Gutiérrez, *et al.,* "Strong isotropic flux pinning in solution-derived $YBa_2Cu_3O_{7-x}$ nanocomposite superconductor films," *Nature Materials*, vol. 6, no. 5, pp. 367-373, May 2007.

[8] B. Maiorov, *et al.,* "Synergetic combination of different types of defect to optimize pinning landscape using $BaZrO_3$-doped $YBa_2Cu_3O_7$," *Nat. Materials*, vol. 8, no. 5, pp. 398-404, May 2009.

[9] S. Wee, *et al.,* "Formation of self-assembled double –perovskite, Ba_2YNbO_6 nanocolumns and their contribution to flux pinning and J_c in Nb-doped $YBa_2Cu_3O_{7-\delta}$ films," *Appl. Phys. Express,* vol. 3, no. 2, pp.023101-1 – 023101-6, 2010.

[10] V. Solovyov, *et al.,* "Influence of defect-induced biaxial strain on flux pinning in thick $YBa_2Cu_3O_7$ layers," *Physical Review B*, vol. 86, no. 9, pp. 004500-1- 004500-4, 2012.

[11] Y. Liu, G. Du, "Preparation and flux-pinning properties of multilayered yttrium barium copper oxide thin films containing alternating barium zirconate and yttria nanostructures," *Journal of Electronic Materials*, vol. 40, no. 7, pp. 1512-1516, 2011.

[12] F. Baca, *et al.,* "Interactive Growth Effects of Rare-Earth Nanoparticles on Nanorod Formation in $YBa_2Cu_3O_x$ Thin Films," *Adv. Funct. Matl.,* vol. 23, no. 38, pp. 4826-4831, Oct. 2013.

[13] M. A. Sebastian, *et al.,* " Optimizing flux pinning of YBCO superconductor with $BaSnO_3$ + Y_2O_3 dual mixed phase additions," *IEEE Trans. on Appl. Supercond.,* vol. 23, no. 3, p.8002104, 2013.

[14] H. Zhou, *et al.,*"Thickness dependence of critical current density in $YBa_2Cu_3O_{7-\delta}$ films with $BaZrO_3$ and Y_2O_3 addition," *Supercond. Sci. Technol*., vol. 22, no. 8, 6pp, 2009.

[15] T. Aytug, *et al.,* "Enhanced flux pinning in MOCVD-YBCO films through Zr additions: systematic feasibility studies," *Supercond. Sci.Technol.,* vol. 23, no. 1, 7pp, 2010.

[16] D. M. Feldmann, *et al.,* "Improved flux pinning in $YBa_2Cu_3O_7$ with nanorods of the double perovskite Ba_2YNbO_6," *Supercond. Sci.Technol.,* vol. 23, no. 9, 6pp, 2010.

[17] S. Foltyn, *et al.,* "Materials science challenges for high-temperature superconducting wire," *Nature Materials*, vol. 6, no. 9, pp. 631-642, Sept. 2007.

[18] M. Peurla, *et al.,* " YBCO films prepared by PLD using nanocrystalline targets doped with $BaZrO_3$ or Y211," *IEEE Trans. on Appl. Supercond.,* vol. 15, no. 2, pp. 3050-3053, 2005.

[19] F. Kametani, Z, Chen, S. I. Kim, A. Gurevich, D. Larbalestier, "Microstructural investigation of the most efficient vortex pinning in a superconducting $YBa_2Cu_3O_{7-\delta}$ thin film," *Microsc. Microanal. ,* vol. 14, suppl. 2, pp342-343, 2008.

[20] S. I. Kim, F. Kametani, Z. Chen, A. Gurevich, D.C. Larbalestier, " On the through-thickness critical current density of an $YBa_2Cu_3O_{7-x}$ film containing a high density of insulating, vortex-pinning nanoprecipitates," *Appl. Phys. Lett.,* vol. 90, no. 252502, pp. 1-3, 2007.

[21] Z. Chen, F. Kametani, A. Gurevich, D. Larbalestier, " Pinning, thermally activated depinning and their importance for tuning the nanoprecipitate size and density in high *Jc* $YBa_2Cu_3O_{7-x}$ films," *Physica C,* vol. 469, no. 23, pp.2021-2028, 2009.

[22] P. Barnes, *et.al.,* "Nanoparticulate flux pinning centers of $YBa_2Cu_3O_{7-\delta}$ films," *IEEE Trans. on Appl. Supercond.,* vol. 17, no. 2, pp.3717-3719, 2007.

[23] T. Haugan, P. N. Barnes, R. Wheeler, F. Meisenkothen, M. Sumption, "Addition of nanoparticle dispersions to enhance flux pinning of the $YBa_2Cu_3O_{7-x}$ superconductor," *Nature,* vol. 430, no. 19, pp. 867-870, 2004.

[24] T. Haugan, *et. al*, "Superconducting Properties of $(M_x/YBa_2Cu_3O_{7-dy})_N$ Multilayer Films with Variable Layer Thickness x", J. Electron. Mater. vol. 36, no. 10, pp. 1234-1242, 2007.

[25] http://www.icdd.com/products/index.html, jcpds pdf #00-040-0159 (YBCO), #00-035-0734 (STO), and #00-038-1434(Y211), #00-041-1105 (Y_2O_3), and #00-055-1002 (BZO).

[26] B. Cullity, S.Stock, Elements of X-Ray Diffraction, 3rd edition, Prentice-Hall Inc., NJ, p. 377, 2001.